# Supporting Information

## Polymer Synergy for Efficient Hole Transport in Solar Cells and Photodetectors

Junwei Liu[1,2,3,6], Zhihua Zhou[1],Yuping Gao[4], Yin Wu[5], Jingjing Wang[1,2,3], Haojin Li[5], Qian Wang[2], Kangkang Zhou[1], Kaihu Xian[1], Yu Chen[8], Wenchao Zhao[9], Fei Zhang[10], Hang Yin[2], Yongsheng Liu[4*], Kui Zhao[5*], Jinyue Yan[6,7*] and Long Ye[1,2,3*]

1. School of Environmental Science and Engineering, School of Materials Science and Engineering, Tianjin Key Laboratory of Molecular Optoelectronic Sciences, Tianjin University, Collaborative Innovation Center of Chemical Science and Engineering (Tianjin), Tianjin, 300350, China.

2. School of Physics and State Key Laboratory of Crystal Materials, Shandong University, Jinan, 250100, China

3. Hubei Longzhong Laboratory, Xiangyang, 441000, China.

4. The Centre of Nanoscale Science and Technology and Key Laboratory of Functional Polymer Materials, Institute of Polymer Chemistry, College of Chemistry and Renewable Energy Conversion and Storage Center (RECAST), Nankai University, Tianjin 300071, China.

5. Key Laboratory of Applied Surface and Colloid Chemistry, Ministry of Education, Shaanxi Key Laboratory for Advanced Energy Devices, Shaanxi Engineering Lab for Advanced Energy Technology, School of Materials Science and Engineering, Shaanxi Normal University, Xi'an 710119, China.

6. Department of Building Environment and Energy Engineering, The Hong Kong Polytechnic University, Kowloon, Hong Kong, China.

7. Future Energy Center, Mälardalen University, Västerås 72123, Sweden.

8. Institute of High Energy Physics, Chinese Academy of Sciences, Beijing 100049, China.

9. Co-Innovation Center of Efficient Processing and Utilization of Forest Resources, College of Materials Science and Engineering, Nanjing Forestry University, Nanjing 210037, China.

10. School of Chemical Engineering and Technology, Tianjin University, Tianjin 300072, China.

*Correspondence: liuys@nankai.edu.cn (Y.L.); zhaok@snnu.edu.cn (K.Z.); jjyan@polyu.edu.hk (J.Y.); yelong@tju.edu.cn (L.Y.)

# 1 Device Fabrication

The commonly used structure, ITO/ZnO/PbS QDs/polymer/$MoO_x$/Ag was employed in this work. The ZnO sol-gel was spin-coated on ITO glass substrates at 3000 rpm for 40 s, and repeated twice, delivering a total thickness of ~100 nm. According to recent reports,[1,2] the prepared PbS QDs in DMF (~1100 mg/mL) were spin-coated on ZnO film to form ~300 nm QD films and were annealed at 75 ℃ for 15 min. For polymers, PTVT-T, and the polymer blends in chloroform/chlorobenzene (1:1) with a concentration of 4 mg/mL were spin-coated on QD active layer at 2000 rpm. Lastly, $MoO_x$/Ag (8 nm/120 nm) anode was thermally evaporated under low pressure ( $< 10^{-4}$ Pa) and the photovoltaic devices have the area of 0.038 $cm^2$ (defined by a metal aperture). On the other hand, the fabrication of perovskite devices was according to our recent reports with proper modification and the photovoltaic devices have the area of 0.1 $cm^2$.[3,4] For polymers, PTVT-T was processed in chloroform/chlorobenzene (1:1) with a concentration of 4 mg/mL and the polymer blends was processed in o-xylene/chlorobenzene (7:3) with the same concentration.

# 2 Characterizations

The UV-vis-NIR absorption spectra were measured by Shimadzu UV-3600 Plus spectrometer. Photoluminescence was measured by the FLIM equipment consisting of the confocal optical microscope (Nanofinder FLEX2, Tokyo Instruments, Inc.). Femtosecond pump-probe TA measurements were following our recent work.[2] Moreover, Keithley 2400 source meter was employed to measure the *J-V* curves under the standard AM 1.5G spectrum with an AAA solar simulator (SS-F5-3A, Enli Technology Co. Ltd, Taiwan). The device performance is tested in the nitrogen atmosphere of the glovebox. The measurements of quantum dot solar cells were done using a voltage step of 0.02 V, a dwell time of 1 ms, a voltage scan range of -0.1 to 0.8 V. Moreover, over 10 individual devices were measured for each polymer HTMs. For thermal stability measurement, the samples were stored on the heating plate with a

temperature of ~85 ℃ in the dark glove box. In addition, Bruker MultiMode 8 AFM in tapping mode and JEOL JEM-2100PLUS electron microscope were employed to collect the AFM and TEM images, respectively. GIWAXS results were measured at beamline 1W1A, Beijing Synchrotron Radiation Facility (BSRF) and the detailed procedures are well documented in our previous reports.[5,6]

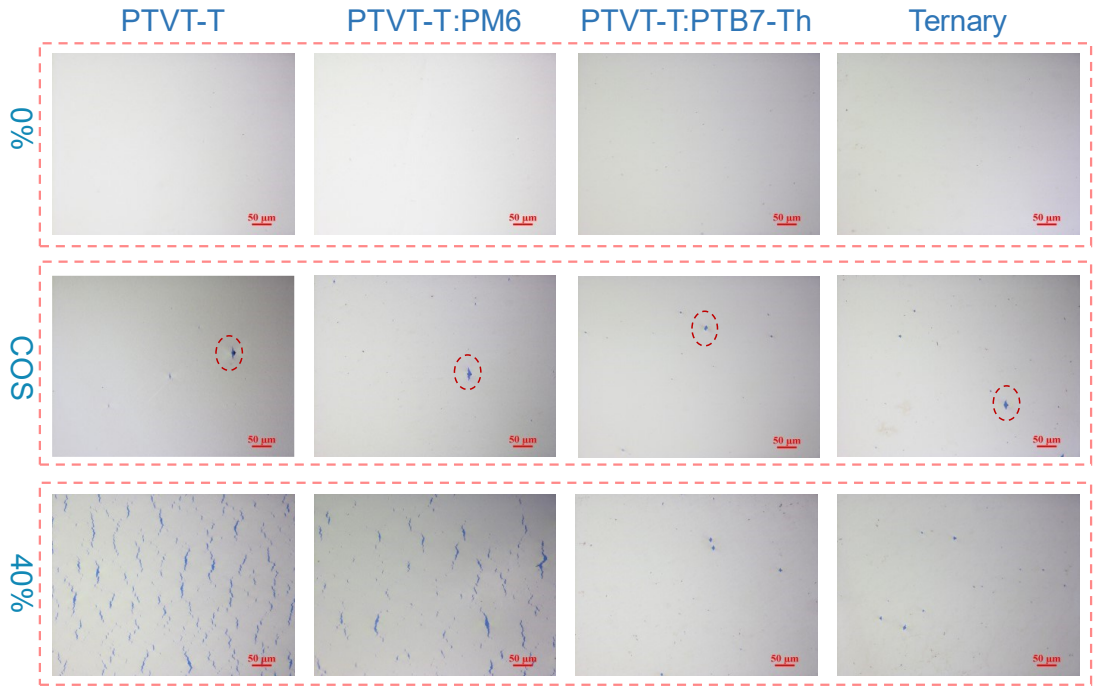


**Figure S1.** Film-on-elastomer tests of PTVT-T, PTVT-T:PM6, PTVT-T:PTB7-Th and the ternary films.

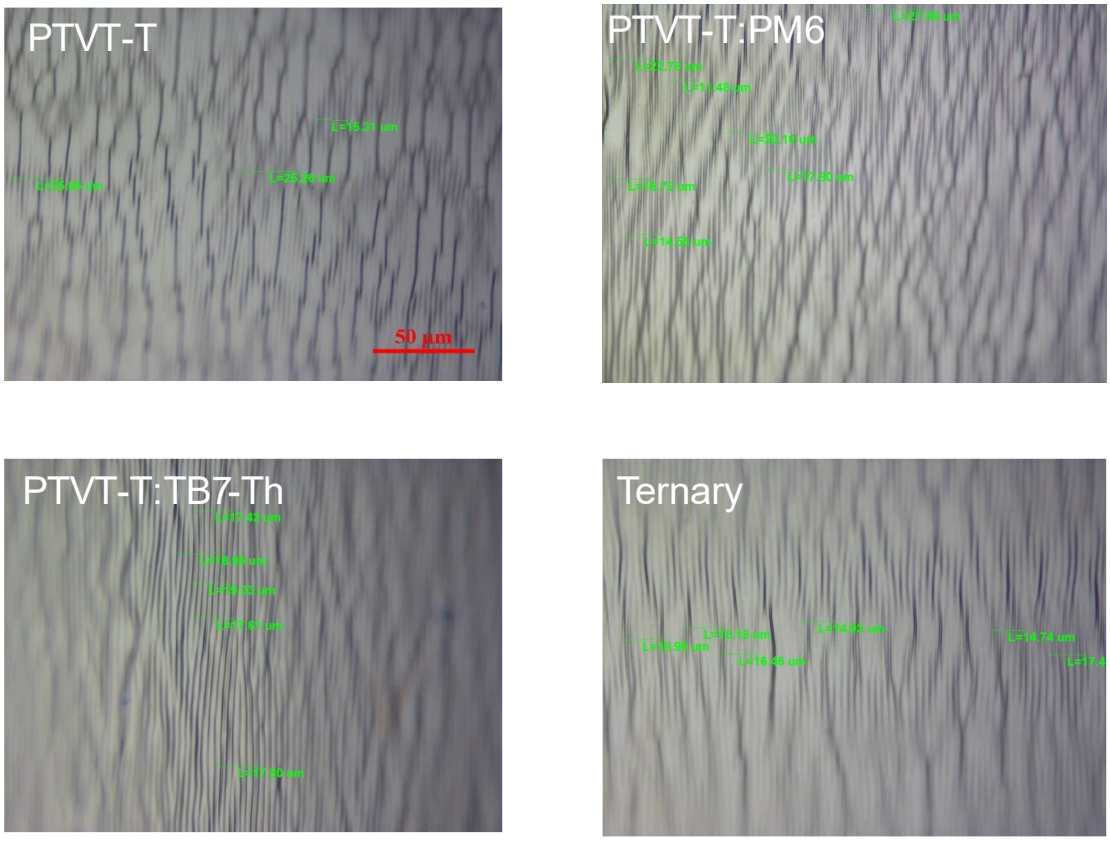


**Figure S2.** Optical micrographs of PTVT-T, PTVT-T:PM6, PTVT-T:PTB7-Th and the ternary films.

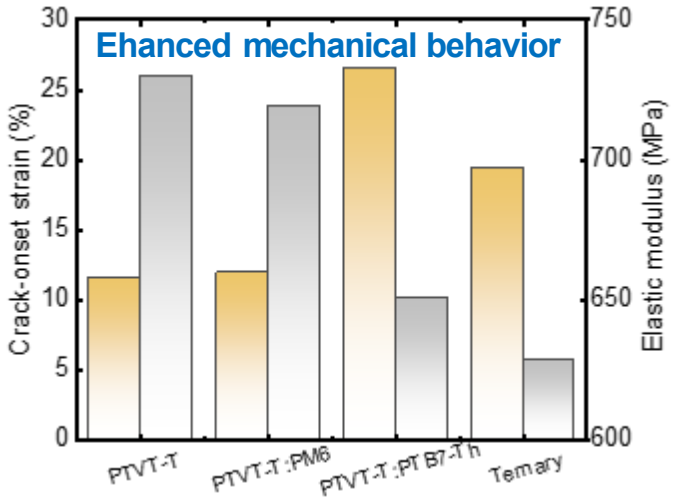


**Figure S3.** The crack onset strains and elastic moduli of PTVT-T, PTVT-T:PM6, PTVT-T:PTB7-Th and the ternary films.

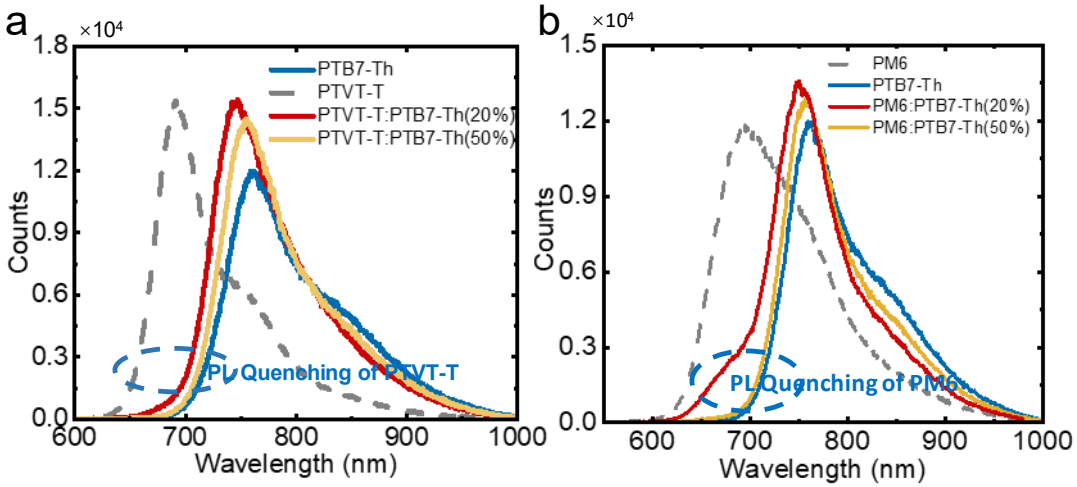


**Figure S4.** Photoluminescence results of PTVT-T (a), PM6 (b), PTB7-Th and the blend films.

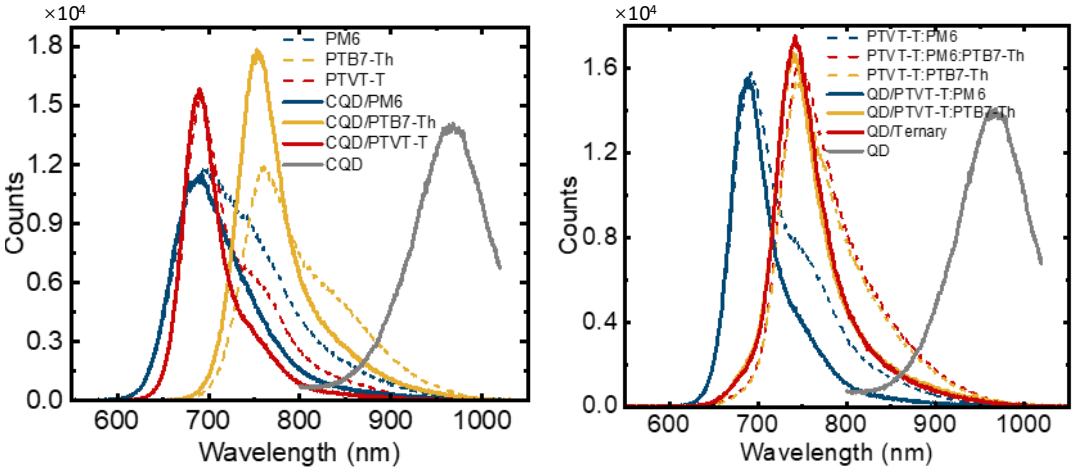


**Figure S5.** Photoluminescence results of QD/polymer heterojunction films, including QD/PM6, QD/PTB7-Th, QD/PTVT-T, QD/PTVT-T:PM6, QD/PTVT-T:PTB7-Th and QD/Ternary films.

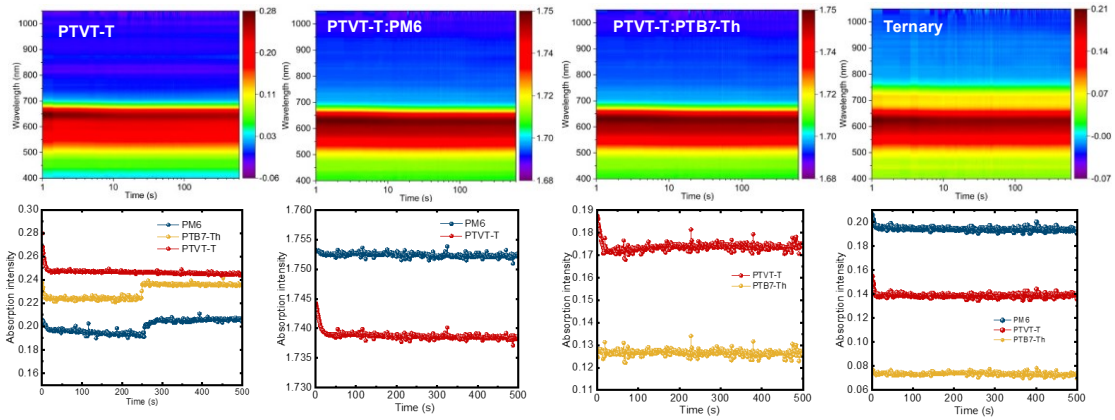


**Figure S6.** In-situ Absorption evolution of PTVT-T, PTVT-T:PM6, PTVT-T:PTB7-Th and Ternary films during the annealing process.

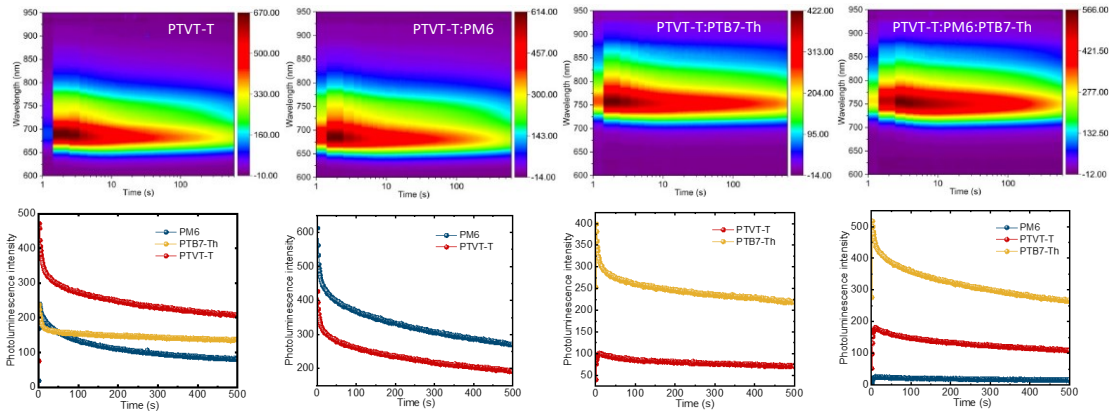


**Figure S7.** In-situ PL evolution of PTVT-T, PTVT-T:PM6, PTVT-T:PTB7-Th and Ternary films during the annealing process.

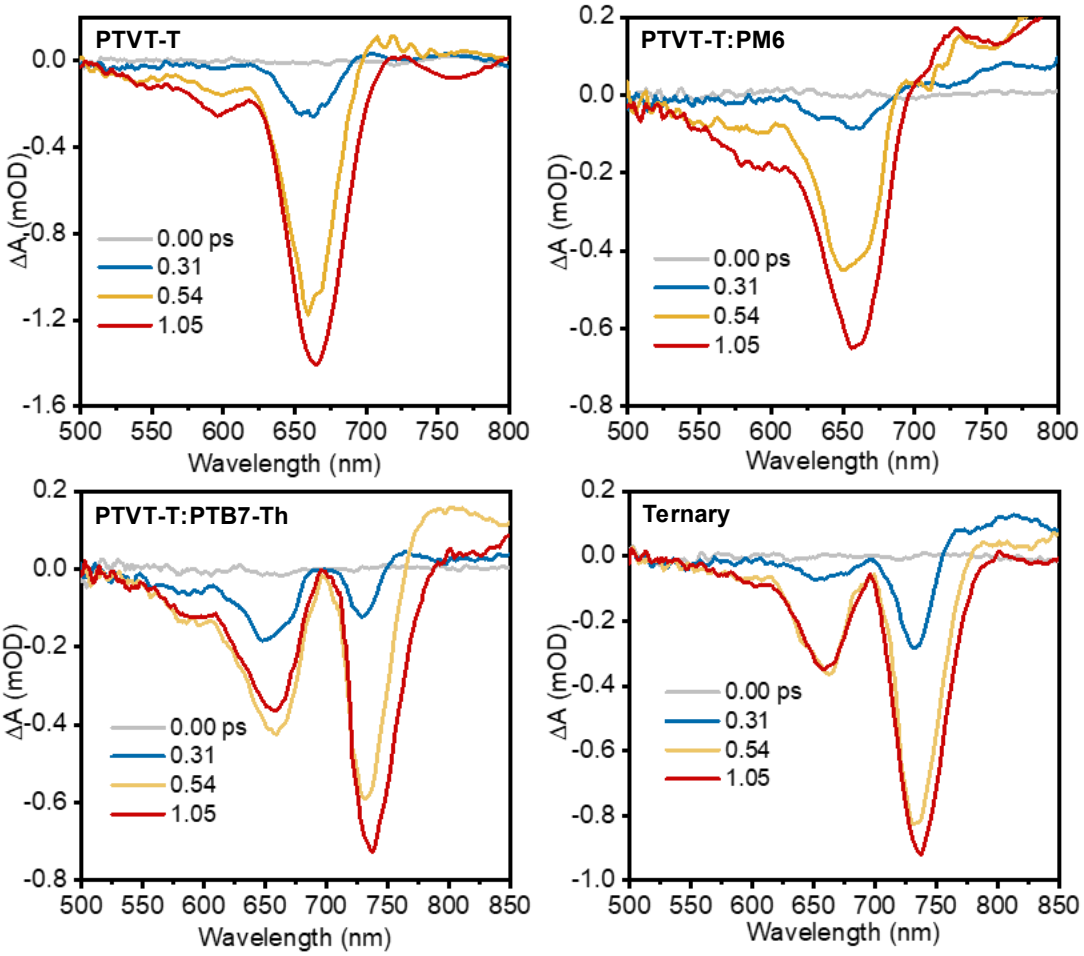


**Figure S8.** Decay spectra of PTVT-T, PTVT-T:PM6, PTVT-T:PTB7-Th and Ternary films.

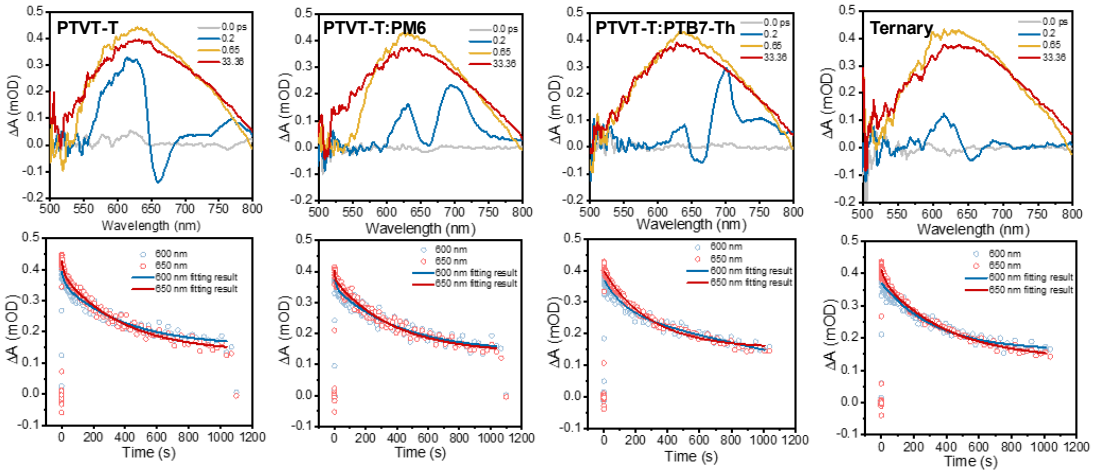


**Figure S9.** Decay spectra and global fitting of QD/polymer heterojunction, including QD/PTVT-T, QD/PTVT-T:PM6, QD/PTVT-T:PTB7-Th and QD/Ternary films.

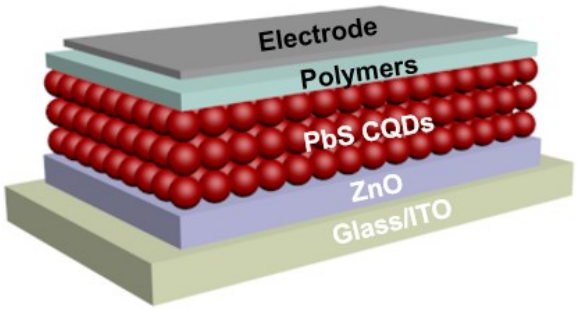


**Figure S10.** Device structure of QD/polymer solar cells and photodetectors.

**Table S1**. Performance of the QD/polymer Solar Cells.

| | $V_{oc}$ (V) | $J_{sc}$ (mA cm$^{-2}$) | FF (%) | PCE (%) |
|---|---|---|---|---|
| PTVT-T | 0.655± 0.010 (0.664) | 27.7 ± 0.58(28.7) | 60.8 ± 1.1 (61.7) | 11.0 ± 0.7 (11.8) |
| PTVT-T:PM6 | 0.674 ± 0.011 (0.682) | 27.9 ± 0.41(28.3) | 62.7 ± 1.1 (63.8) | 11.8 ± 0.4 (12.3) |
| PTVT-T:PTB7-Th | 0.644 ± 0.010(0.655) | 28.6 ± 0.38(28.9) | 65.2± 1.1 (66.1) | 12.0 ± 0.6 (12.5) |
| Ternary | 0.667 ± 0.012 (0.679) | 29.1 ± 0.32(29.4) | 66.1± 1.2 (67.5) | 12.8 ± 0.6 (13.5) |

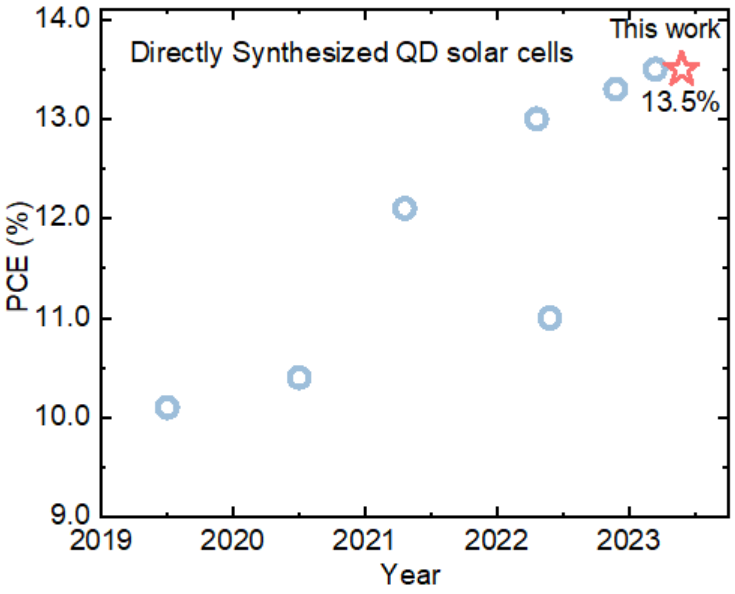


**Figure S11.** PCE progress of directly-synthesized PbS QD solar cells.

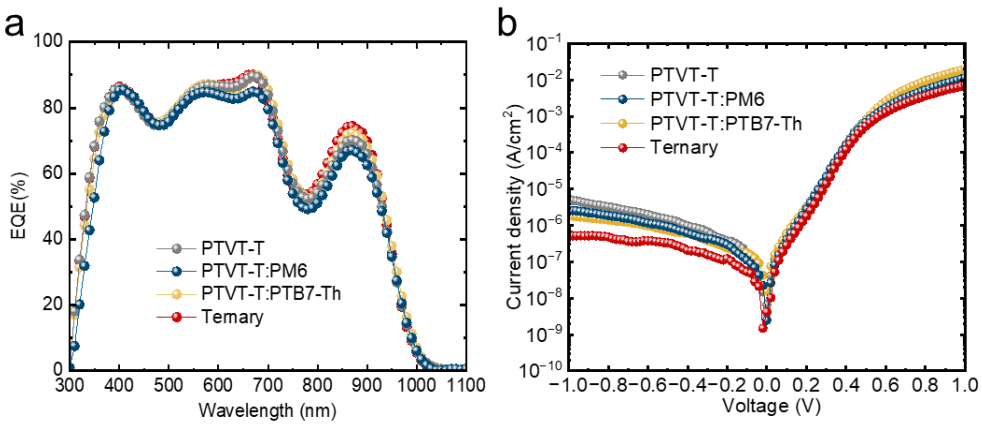


**Figure S12.** External quantum efficiency (a) and dark current density (b) of QD/polymer photodiode devices.

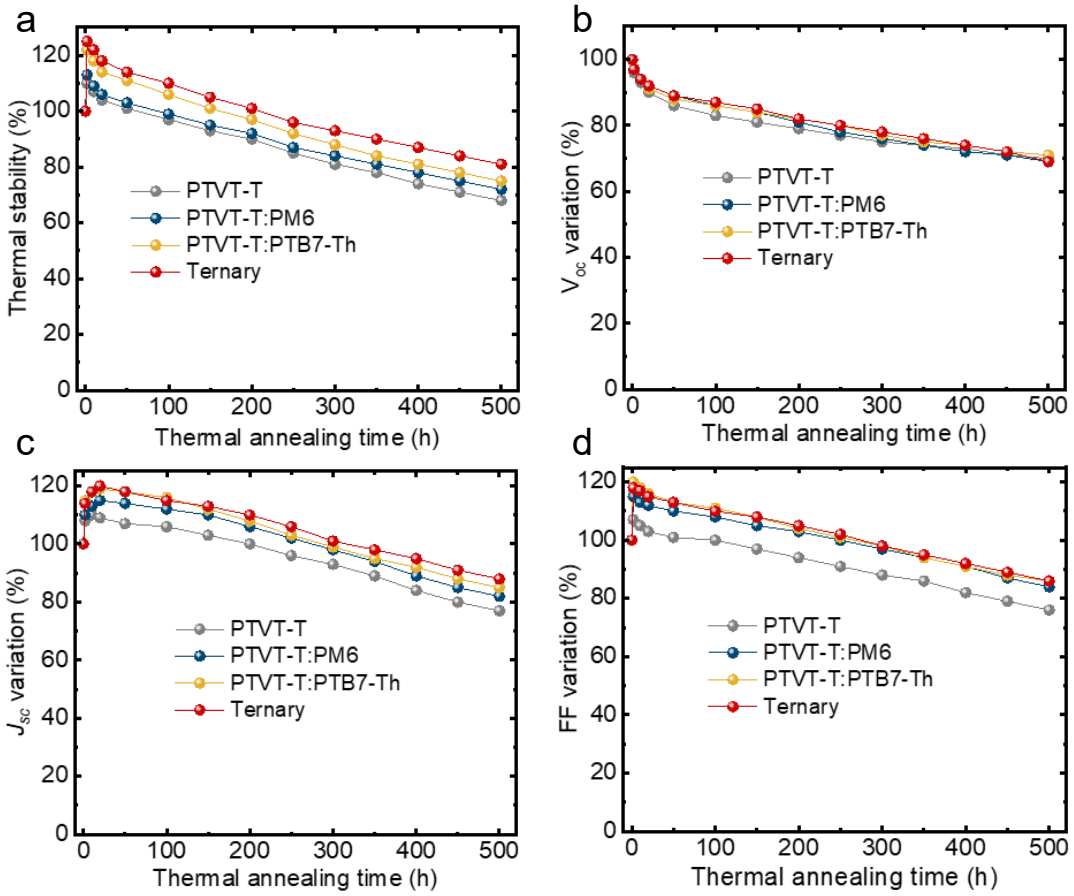


**Figure S13.** (a-d) PCE, $V_{oc}$, $J_{sc}$ and FF evolution of QD/polymer solar cells, respectively.

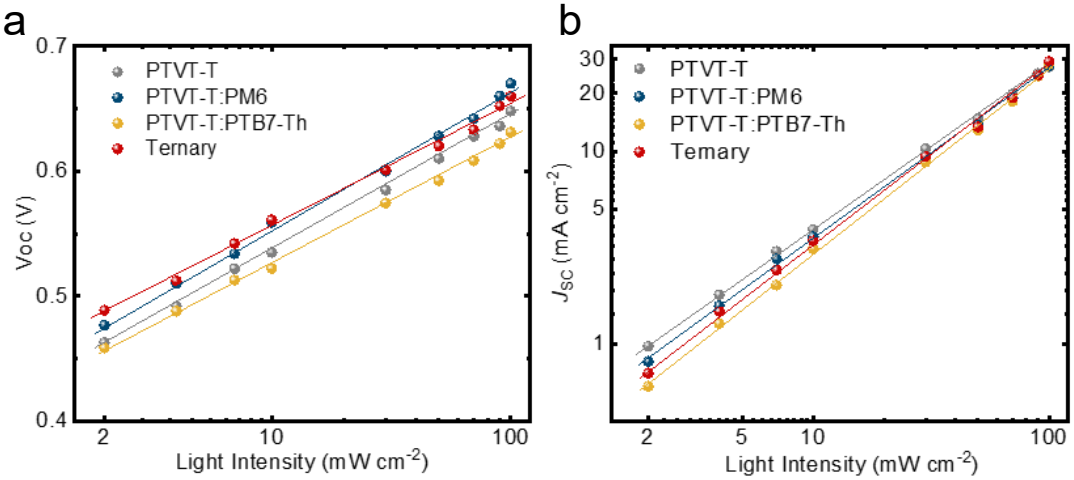


**Figure S14.** Light-intensity dependence of $V_{oc}$ (a) and $J_{sc}$ (b) of QD/polymer devices.

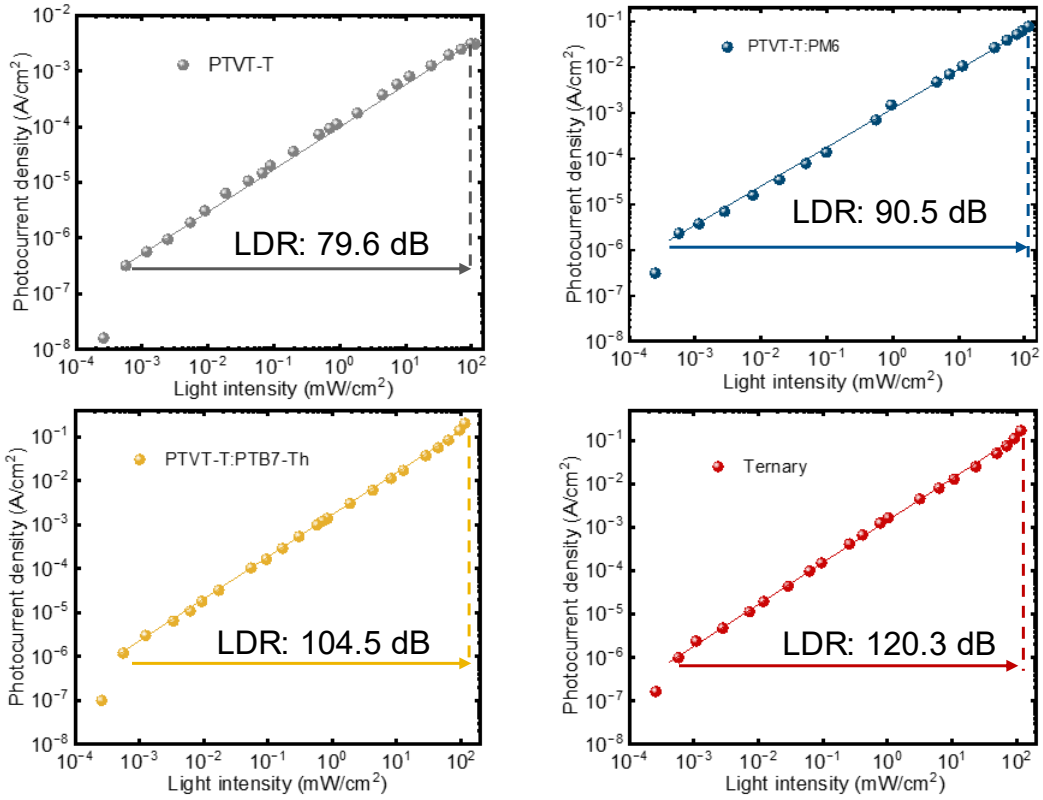


**Figure S15.** Linear dynamic range of QD/polymer photodetectors.

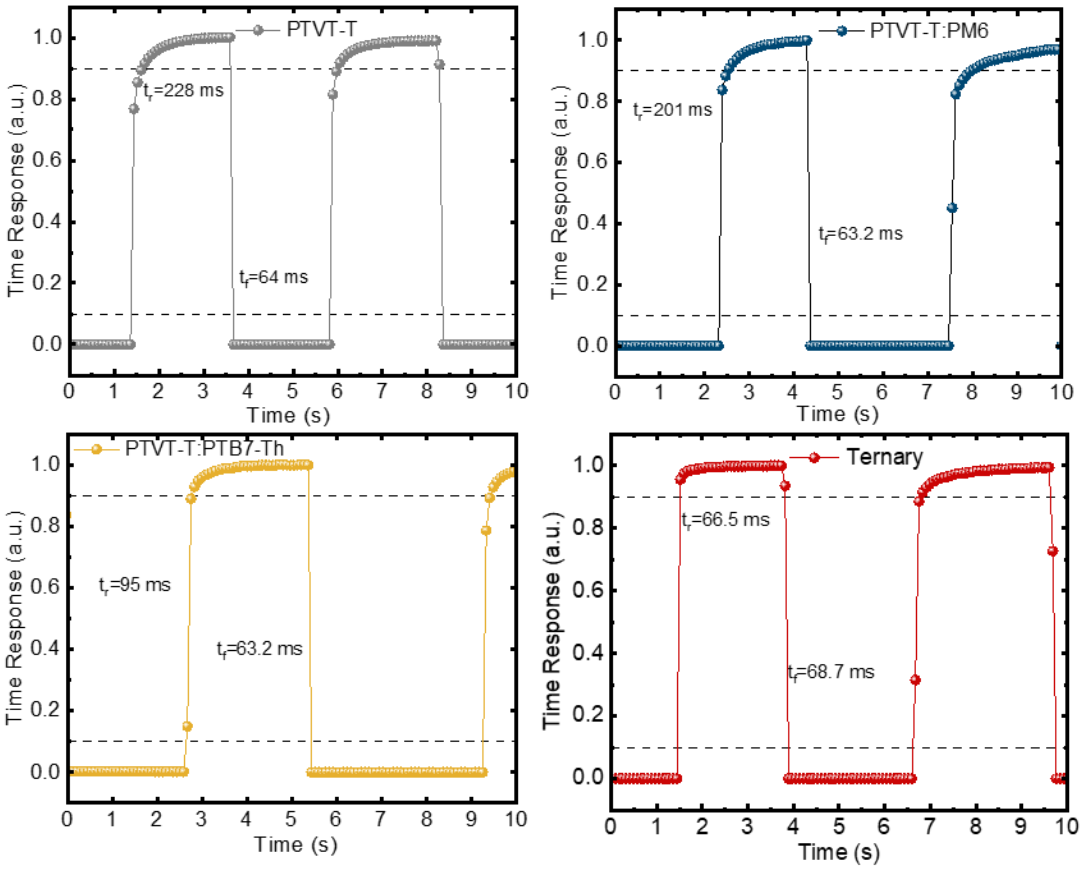

**Figure S16.** Response speed of QD/polymer photodetectors.

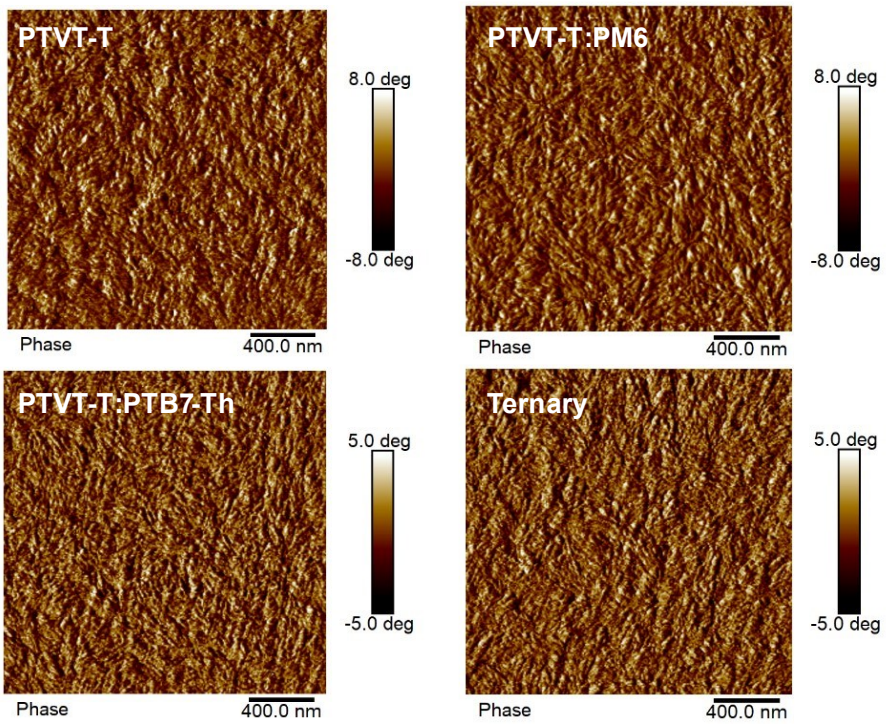


**Figure S17.** AFM phase images of PTVT-T, PTVT-T:PM6, PTVT-T:PTB7-Th and the ternary films.

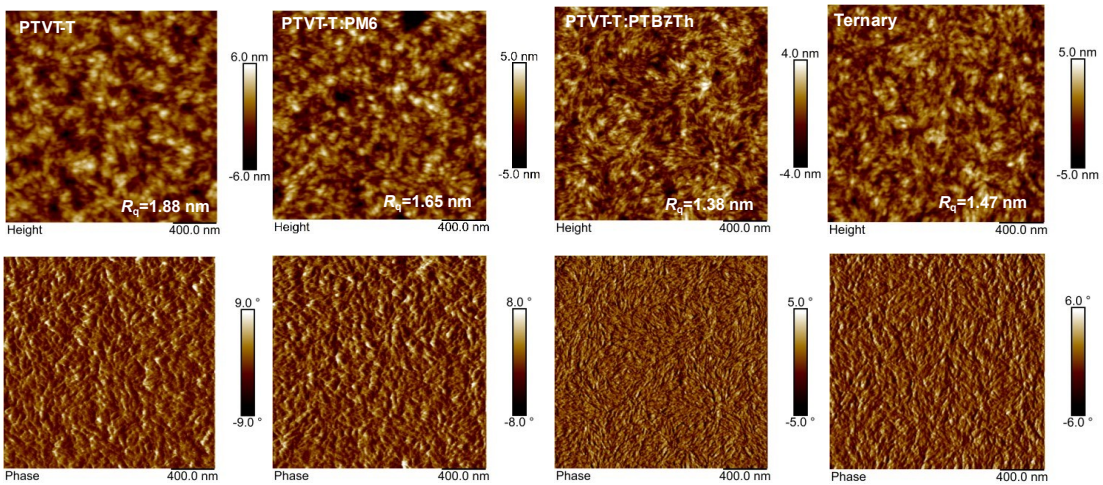


**Figure S18.** AFM images of PTVT-T, PTVT-T:PM6, PTVT-T:PTB7-Th and the ternary films after annealing.

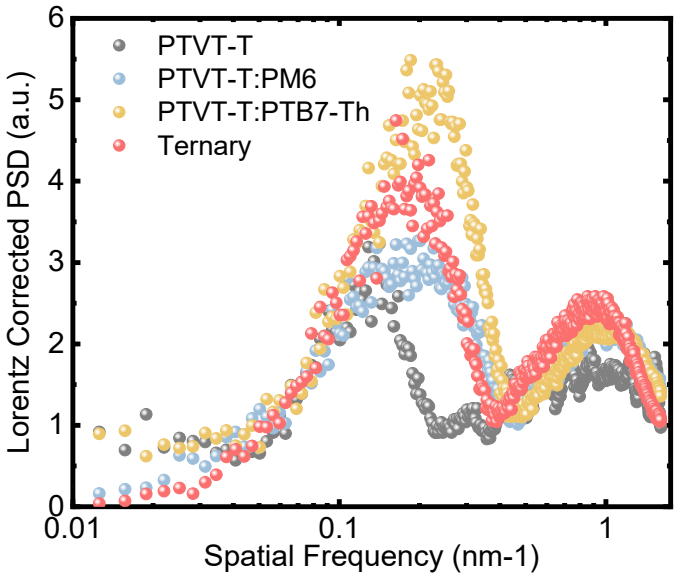


**Figure S19.** PSD profiles of PTVT-T, PTVT-T:PM6, PTVT-T:PTB7-Th and the ternary films.

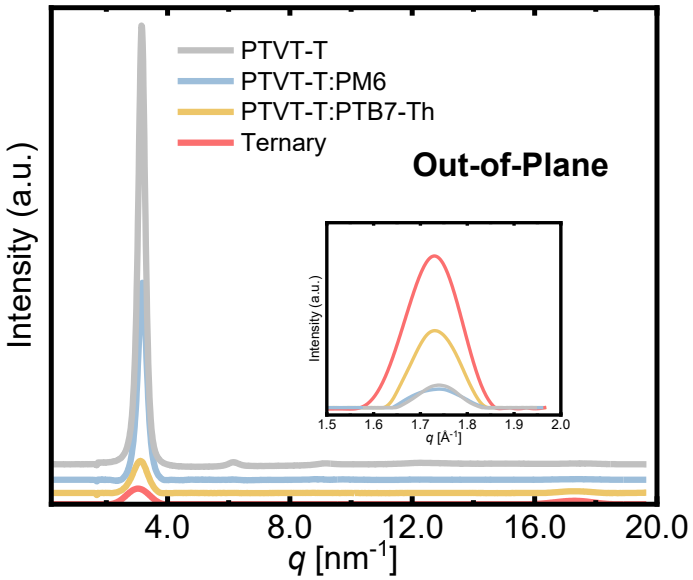


**Figure S20.** 1D in-plane scattering profile of PTVT-T, PTVT-T:PM6, PTVT-T:PTB7-Th and the ternary films.

**Table S2**. Performance of the perovskite/polymer Solar Cells at forward scan.

| | $V_{oc}$ (V) | $J_{sc}$ (mA cm$^{-2}$) | FF (%) | PCE (%) |
|---|---|---|---|---|
| PTVT-T | 1.080± 0.016 (1.092) | 19.7 ± 0.65 (20.1) | 67.4 ± 1.5 (68.6) | 14.3 ± 0.8 (15.1) |
| PTVT-T:PM6 | 1.173 ± 0.013 (1.182) | 23.3± 0.59 (23.7) | 72.5 ± 1.2 (73.5) | 19.8 ± 0.6 (20.6) |
| PTVT-T:PTB7-Th | 1.124 ± | 23.0 ± 0.45(23.6) | 74.5± 1.4 (75.8) | 19.3 ± 0.7 |

| | | | | |
|---|---|---|---|---|
| | 0.017(1.138) | | | (20.3) |
| Ternary | 1.159 ± 0.012 (1.162) | 24.3 ± 0.52(24.7) | 77.8± 1.3 (79.0) | 22.0 ± 0.6 (22.7) |

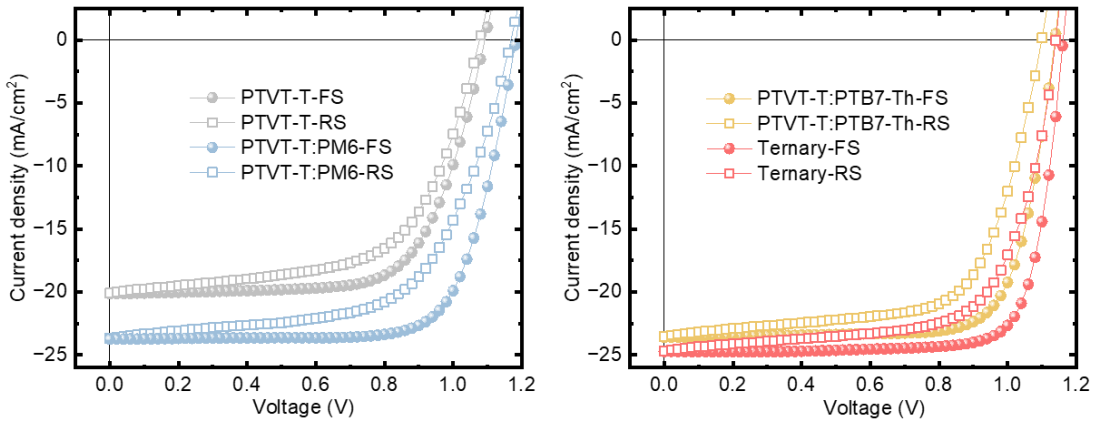


**Figure S21.** Hysteresis measurement. Perovskite photovoltaic performance and J-V measurements with a reverse scan (RS) (1.2 V-0 V, step 0.02 V) and forward scan (RS) (0 V-1.2 V, step 0.02 V).

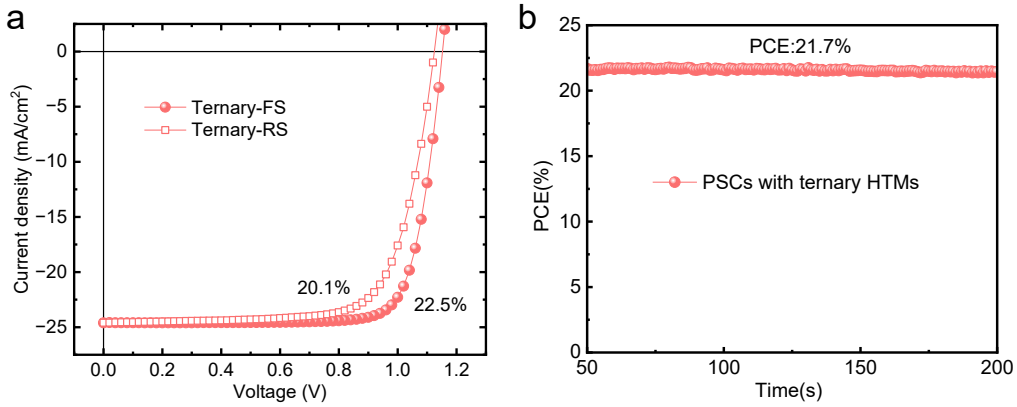


**Figure S22.** (**a**) Perovskite photovoltaic performance based on ternary HTMs and the corresponding *J-V* measurements with a reverse scan (RS) (1.2 V-0 V, step 0.02 V) and forward scan (RS) (0 V-1.2 V, step 0.02 V) with the slight reduction of hysteresis. (**b**) The steady output of perovskite solar cells based on ternary HTMs.

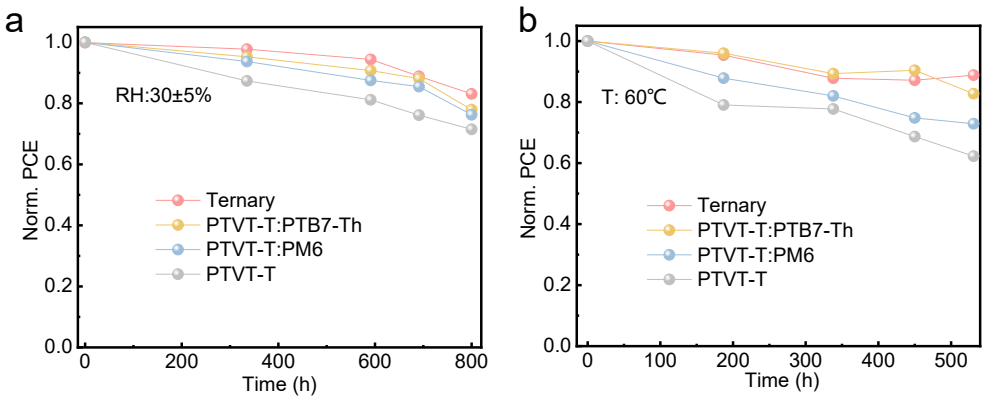


**Figure S23.** Stability of perovskite solar cells at the relative humidity of 30% (a) and the heating temperature of 60 ℃ (b).

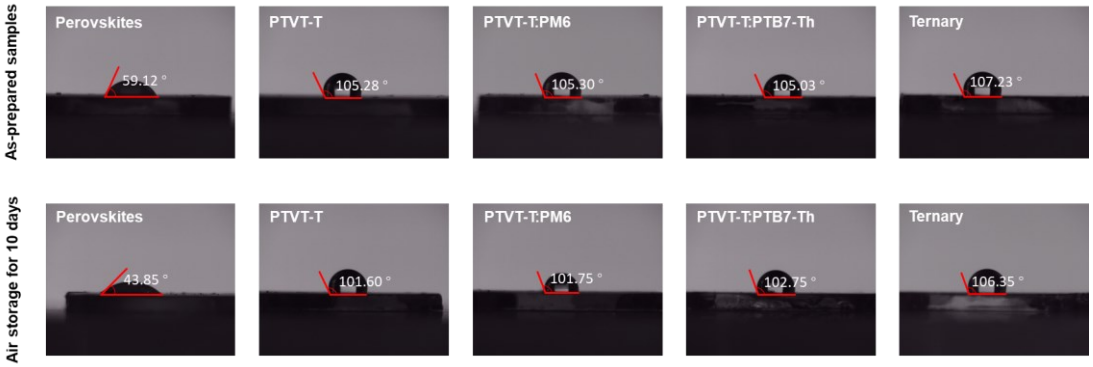


**Figure S24.** The characterizations of perovskite/polymer solar cells under air storage via contact angle measurement.

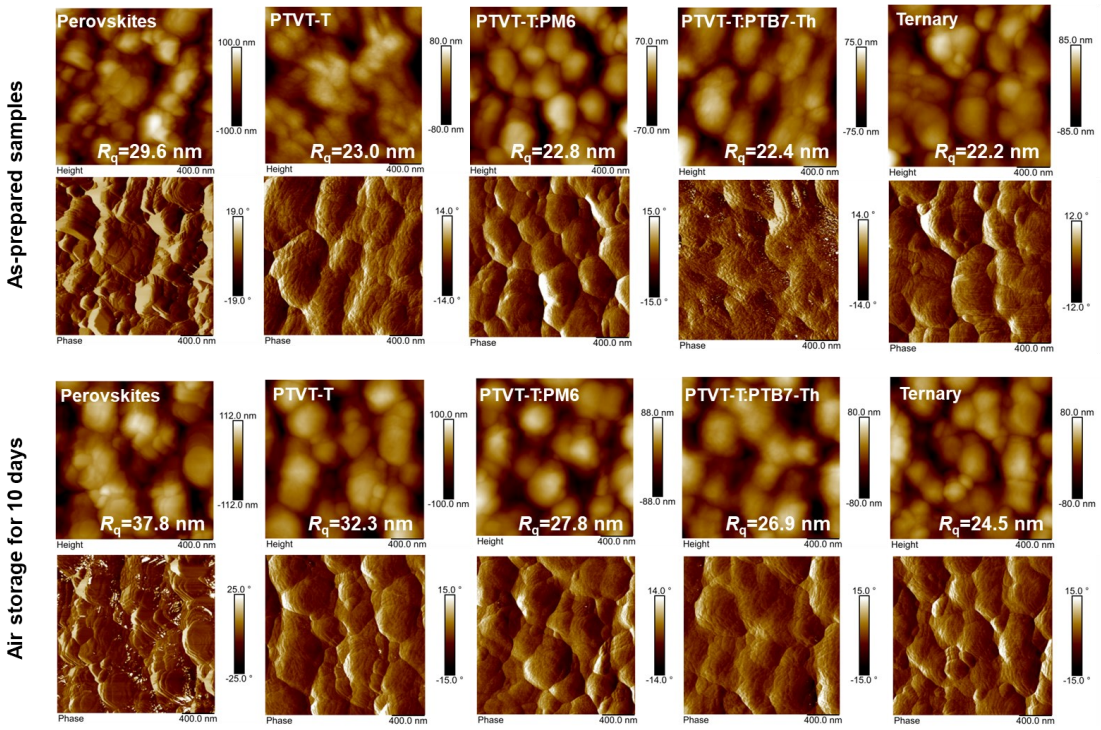


**Figure S25.** The stability characterizations of perovskite/polymer solar cells under thermal annealing via AFM morphology.

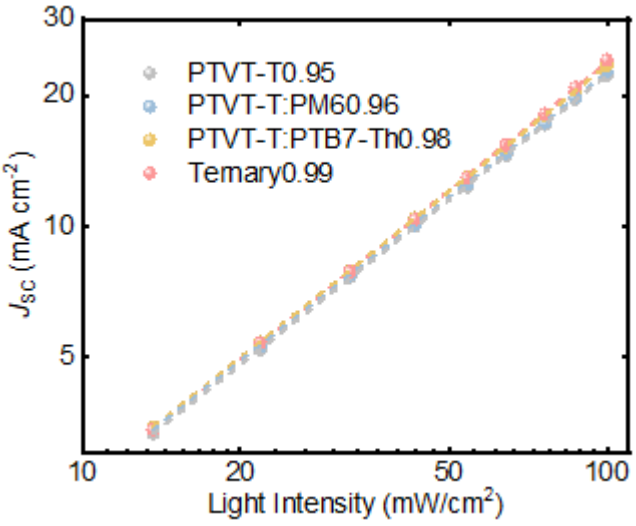


**Figure S26.** Light-intensity dependence of $J_{sc}$ for perovskite solar cells.

# References


1 F. Li, Y. Liu, G. Shi, W. Chen, R. Guo, D. Liu, Y. Zhang, Y. Wang, X. Meng, X. Zhang, Y. Lv, W. Deng, Q. Zhang, Y. Shi, Y. Chen, K. Wang, Q. Shen, Z. Liu, P. Müller-Buschbaum and W. Ma, *Adv. Funct. Mater.*, 2021, **31**, 2104457.

2 J. Liu, Y. Liu, J. Wang, H. Li, K. Zhou, R. Gui, K. Xian, Q. Qi, X. Yang, Y. Chen, W. Zhao, H.

Yin, Kui Zhao, Zhihua Zhou and Long Ye, *Adv. Energy Mater.*, 2022, **12**, 2201975.

3 Q. Fu, H. Liu, S. Li, T. Zhou, M. Chen, Y. Yang, J. Wang, R. Wang, Y. Chen and Y. Liu, *Angew. Chemie - Int. Ed.*, 2022, **61**, e202210356.

4 Q. Fu, X. Tang, H. Liu, R. Wang, T. Liu, Z. Wu, H. Y. Woo, T. Zhou, X. Wan, Y. Chen and Y. Liu, *J. Am. Chem. Soc.*, 2022, **144**, 9500–9509.

5 K. Zhou, K. Xian, Q. Qi, M. Gao, Z. Peng, J. Liu, Y. Liu, S. Li, Y. Zhang, Y. Geng and L. Ye, *Adv. Funct. Mater.*, 2022, **32**, 2201781.

6 K. Xian, Y. Liu, J. Liu, J. Yu, Y. Xing, Z. Peng, K. Zhou, M. Gao, W. Zhao, G. Lu, J. Zhang, J. Hou, Y. Geng and L. Ye, *J. Mater. Chem. A*, 2022, **10**, 3418–3429.